Supporting Information

Roll-to-roll prelithiation of Sn foil anode suppresses gassing and enables stable full-cell cycling of lithium ion batteries

Hui Xu[1,2†], Sa Li[1,2†*], Can Zhang[1,2], Xinlong Chen[1,2], Wenjian Liu[1,2], Yuheng Zheng[1,2], Yong Xie [1,2], Yunhui Huang[1,2*] and Ju Li[3*]

[1]School of Materials Science and Engineering, Tongji University, Shanghai 201804, China
[2]Institute of New Energy for Vehicles, Tongji University, Shanghai 201804, China
[3]Department of Nuclear Science and Engineering and Department of Materials Science and Engineering, Massachusetts Institute of Technology, Cambridge, MA 02139, USA
[†]These authors contributed equally to this work

Email address: lisa@tongji.edu.cn (SL); huangyh@tongji.edu.cn (YH); liju@mit.edu (JL)

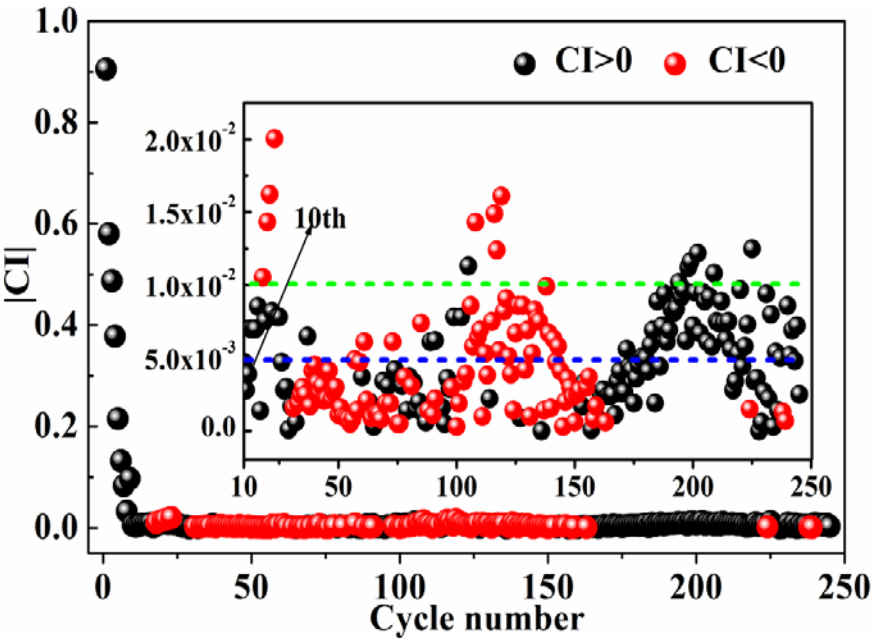

Figure S1. Initial Coulombic inefficiency (ICE≡1-CE) analysis of Sn//Li half-cell. The black dot represents Coulombic inefficiency (CI) >0 and the red dot is CI<0. In the inset, the green dotted line represents CI=0.01, and the blue dotted line represents CI=0.005. We shockingly found that the ICE of Sn anode is up to ~90%. However, after the first cycles, CI drops below 0.005 (the blue dotted line) and the cell can stably cycle more than 250 cycles, which signifies Sn foil may be a potential anode material for LIBs.

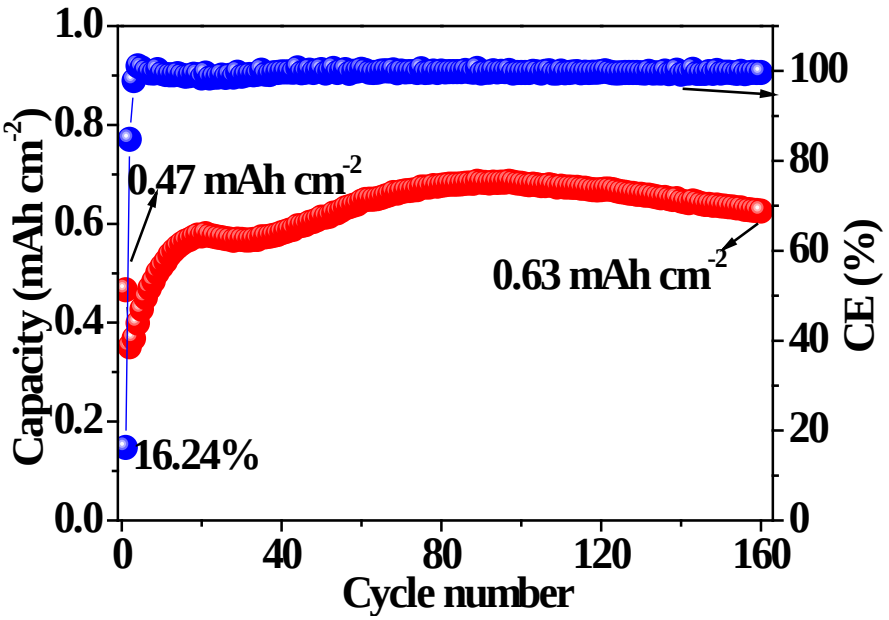

Figure S2. Cycle performance and Coulombic efficiency (CE) of LFP//Sn full cell. The red dot represents capacity and the blue one represents CE. The capacity density of LFP cathode is ~2.65 mAh cm^{-2}. Surprisingly, the first discharge capacity is just 0.47 mAh cm^{-2} and CE is just ~16.24%. This result indicates the serious side reactions also occurred in LFP//Sn full cell.

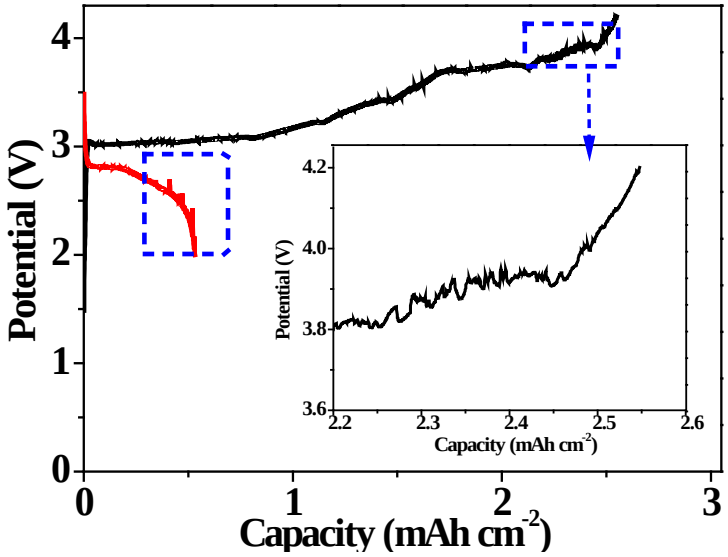

Figure S3. Potential-capacity profile of LFP//Sn full cell. The black one is charge process and the red is the discharge process. The fluctuating potential at final charge and discharge may be caused by gassing.

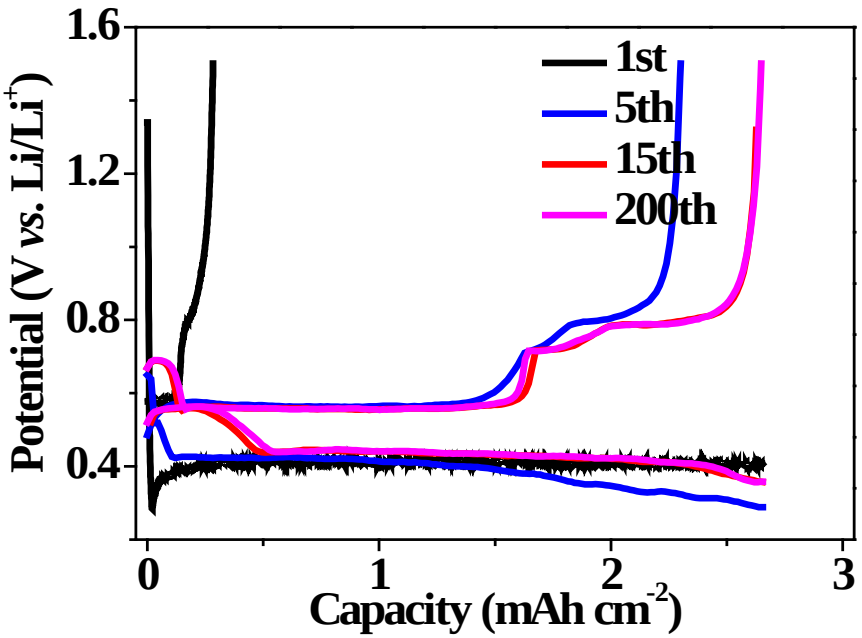

Figure S4. Potential-capacity profile of Sn//Li half-cell. The lines of 15th (the red) and 200th (the pink) are almost overlapped by each other, demonstrating the stability of Sn foil is excellent after initial activation.

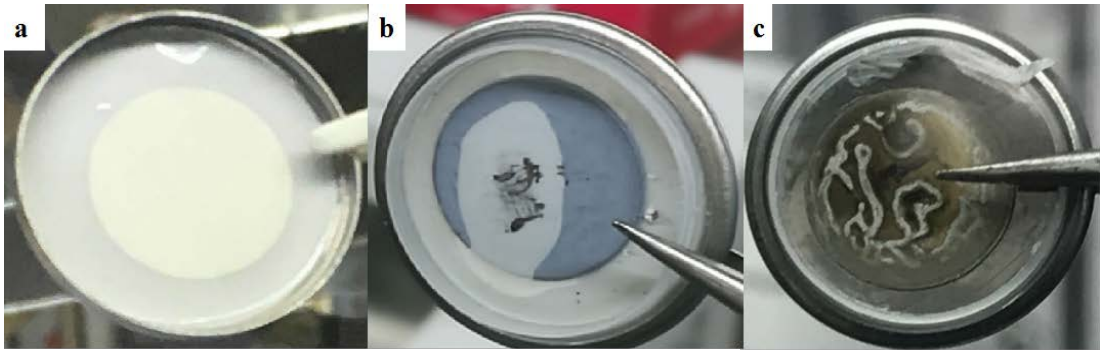

Figure S5. Visual images of gassing generation in Sn//Li coin cell. a, The electrolyte is just dropped into a cell, and the separator is well wetted. **b,** After the 1st cycle, a continuous bubble is located between the separator and Sn surface. **c,** The surface of cycled Sn electrode shows bulging as well as flat region due to the extremely inhomogeneous reactions.

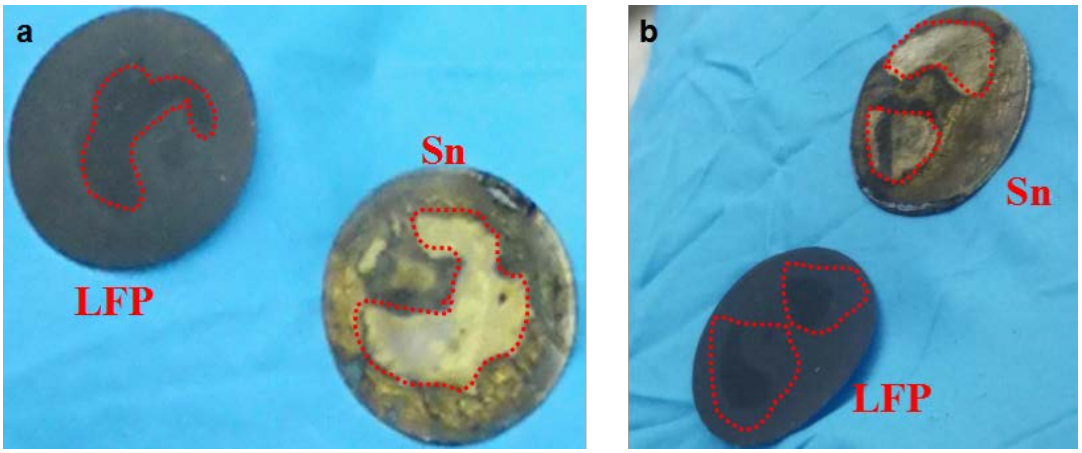

Figure S6. Visual images of gassing generation in LFP//Sn full cells. a,b The cycled LFP and Sn foil electrodes. There are symmetric footprints on the surface of LFP and Sn foil electrodes. Gas isolates electrolyte and stops electrochemical reactions in the region of red circles.

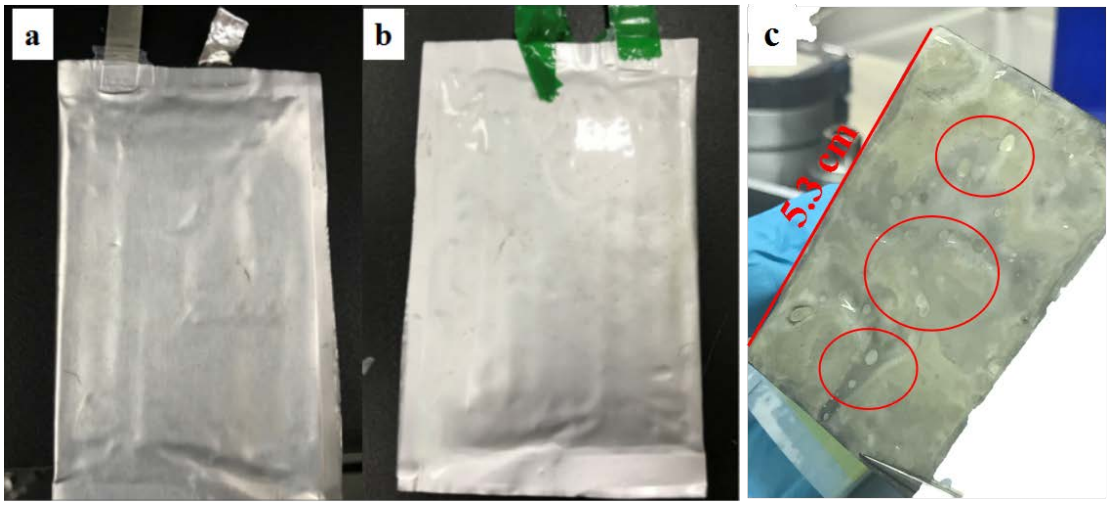

Figure S7. Visual images of gassing generation in a $LiCoO_2$//Sn pouch cell. a, The fresh pouch cell. **b,** The charged pouch cell. There is obvious swelling phenomenon. **c,** The cycled Sn foil electrode of the pouch. There are a number of bubble footprints on the Sn surface, indicating there was indeed serious gassing behavior.

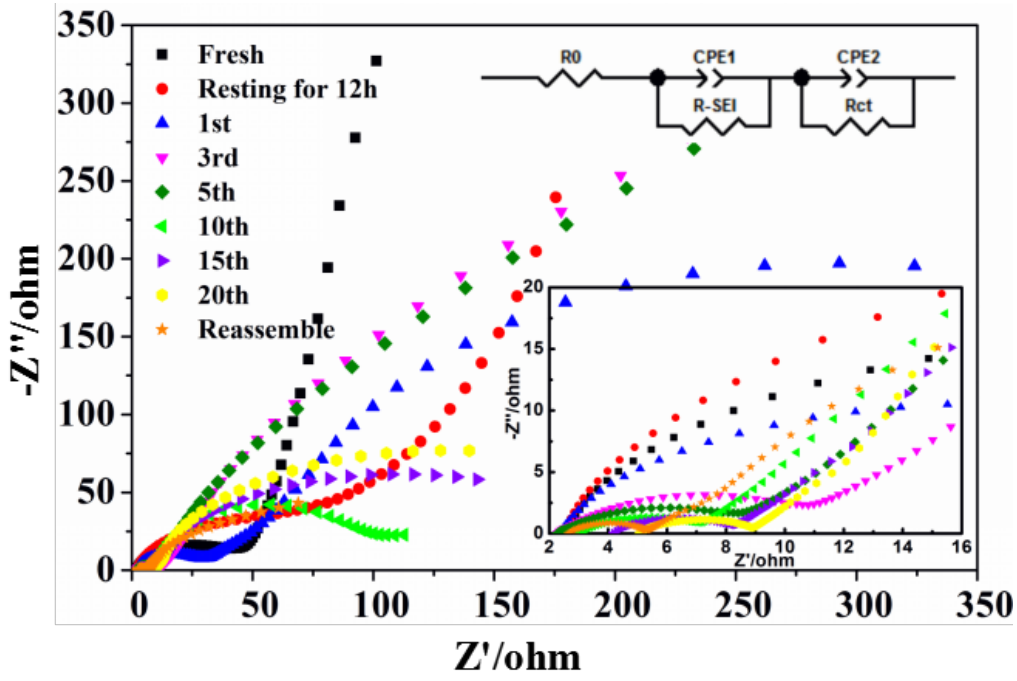

Figure S8. EIS analysis of Sn//Li half-cell. The resistance rises drastically after the first cycles and then declines, which is because the gassing is most serious during first cycles and it declines after SEI formation. After reassembling the cells to drive the gasses out of the system, the impedance becomes smaller again.

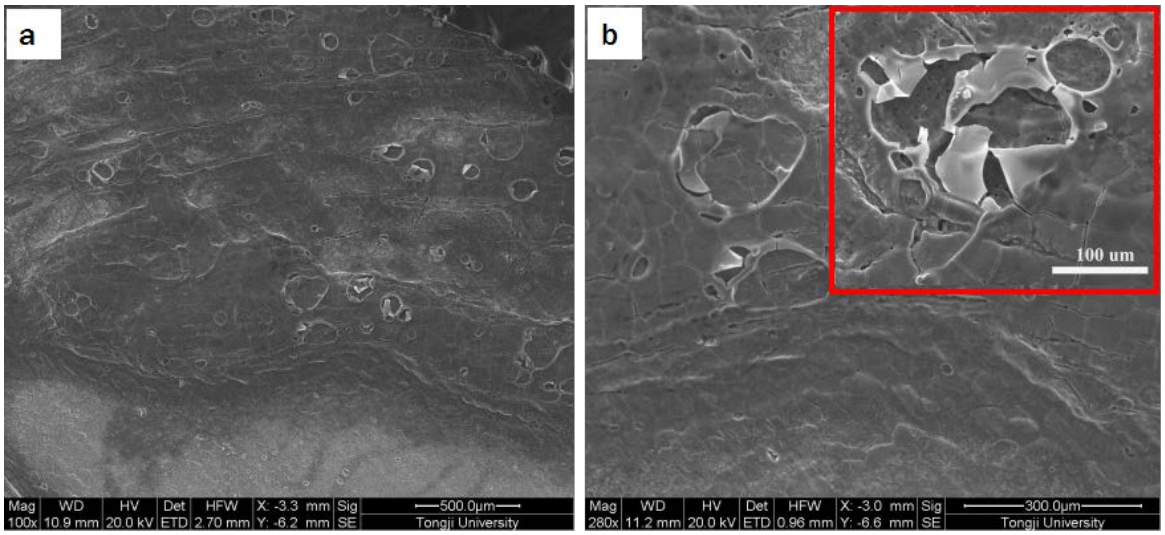

Figure S9. Surface morphology of Sn foil that is just cycled once. a, Low magnification. **b,** High magnification. As shown in the red square, there is massive broken SEI film which is caused by bubbles bursting.

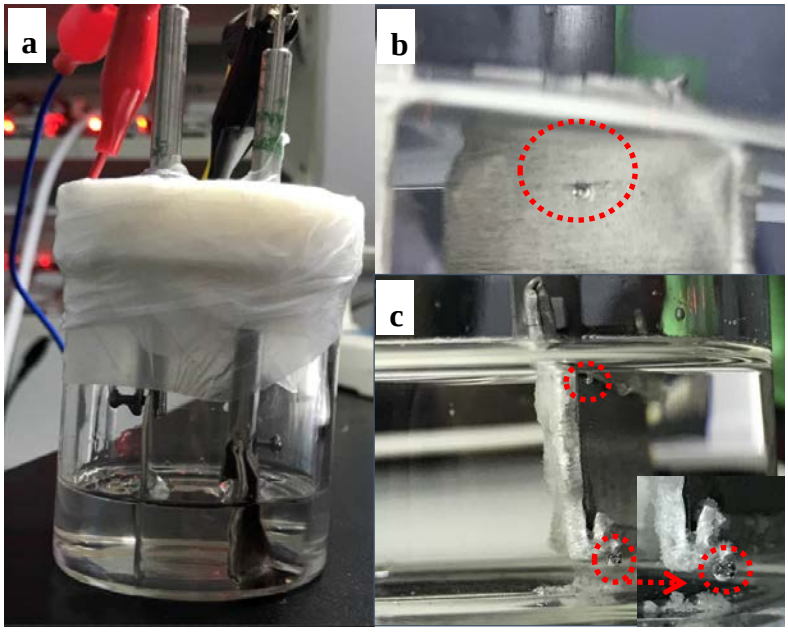

Figure S10. Visual images of beaker battery and gas bubble. a, Setup of home-made beaker battery, including a glass electrolytic cell and two electrodes. One is Sn foil (work electrode) and the other one is lithium foil (counter electrode and reference electrode). The electrolyte is 1M $LiPF_6$ in EC/DEC (V/V=1:1) with 1% VC, 10% FEC. **b, c,** Visual images of bubble: the bubble generation is at 1.5 ~1 V *vs.* Li/Li^+ during lithiation process (b) and the size of bubble is ~1000 μm (c).

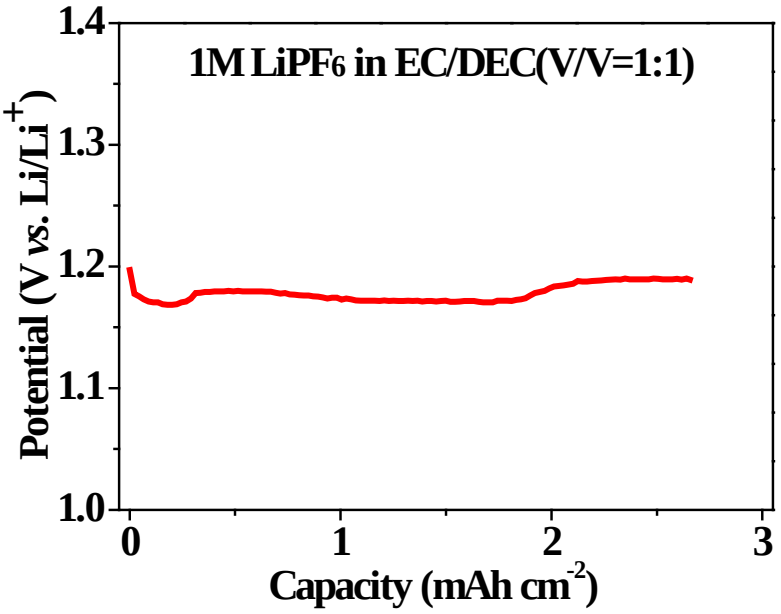

Figure S11. Potential-capacity profile of the beaker cell. The potential maintains at ~1.15 V vs. Li/Li^+, which is due to the sufficient electrolyte (tens of milliliters) that was able to continuously decompose. Since almost all of electrons are consumed in side reactions, Li^+ cannot insert into Sn.

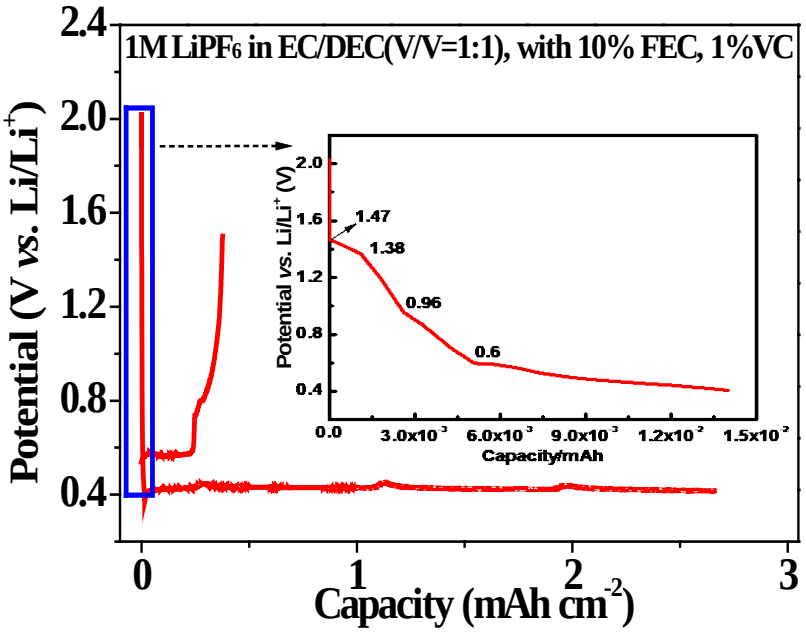

Figure S12. Potential-capacity profile of Sn//Li cell. The electrolyte (~30 μl) is decomposed immediately after lithiating Sn foil. Although the apparent voltage drops fast, the absolute potential of Sn still keeps at a high value.

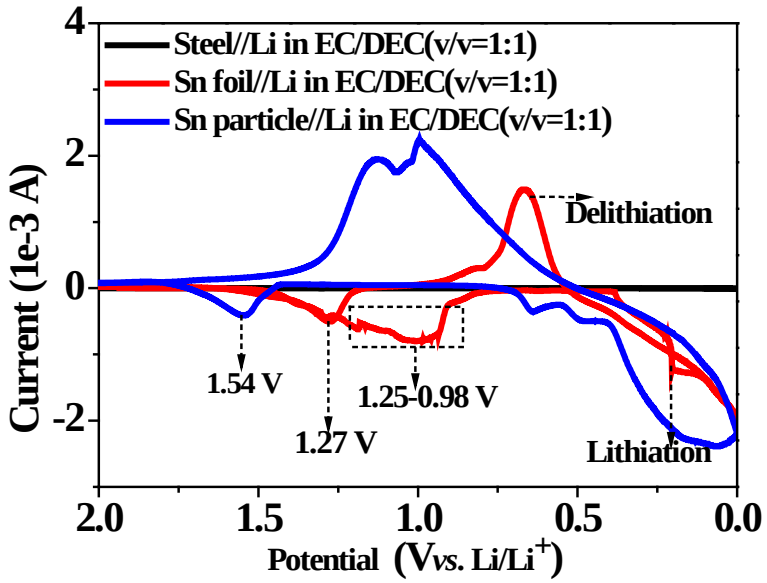

Figure S13. CV results of Sn foil and Sn powder anode. The black is steel//Li symmetrical cell, which almost is a closed straight line, indicating the electrolyte is quite stable at the range of voltage (0-2.2 V vs. Li/Li^+). The red line is Sn//Li half-cell. There is a peak at 1.25~0.98 V on the red line when the cell was negative sweeping (from 2.2 to 0 V), which is related with gassing. Another peak is at 1.27 V when positive sweeping, which may be caused by broken SEI and the re-exposed fresh Sn in the electrolyte. The blue line is Sn powder//Li half-cell. The peak at 1.54 V is caused by the decomposition of VC or FEC.

There are no other peaks because Sn nano-particle is separated from electrolyte by conductive agent and binder.

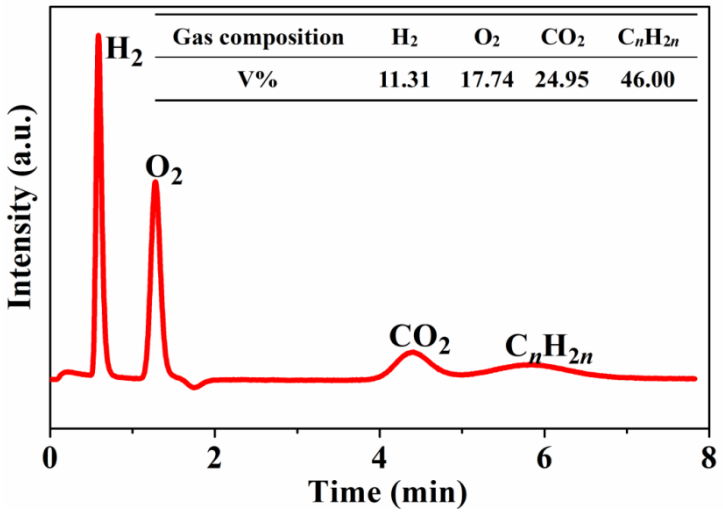

Figure S14. Gas chromatography-mass spectrometry (GCMS) result of $LiCoO_2$//Sn pouch cell. The generation of H_2, CO_2 and C_nH_{2n} are caused by the electrolyte decomposition. And O_2 is from $LiCoO_2$ cathode.

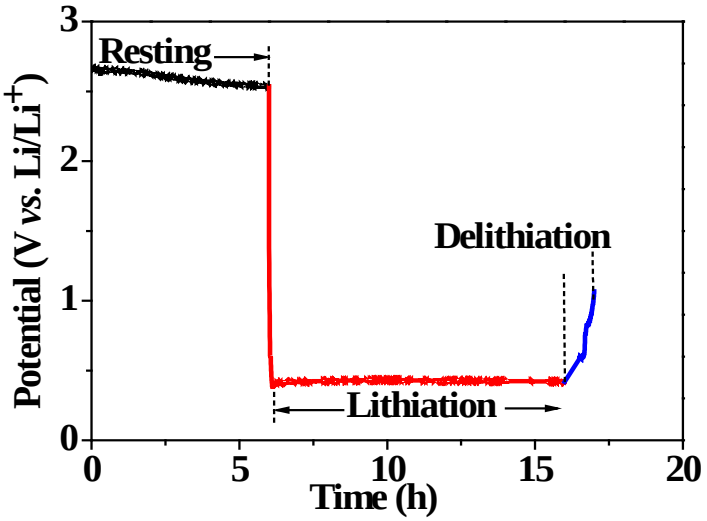

Figure S15. Potential-time profile of Sn//Li cell of in-situ DEMS test.

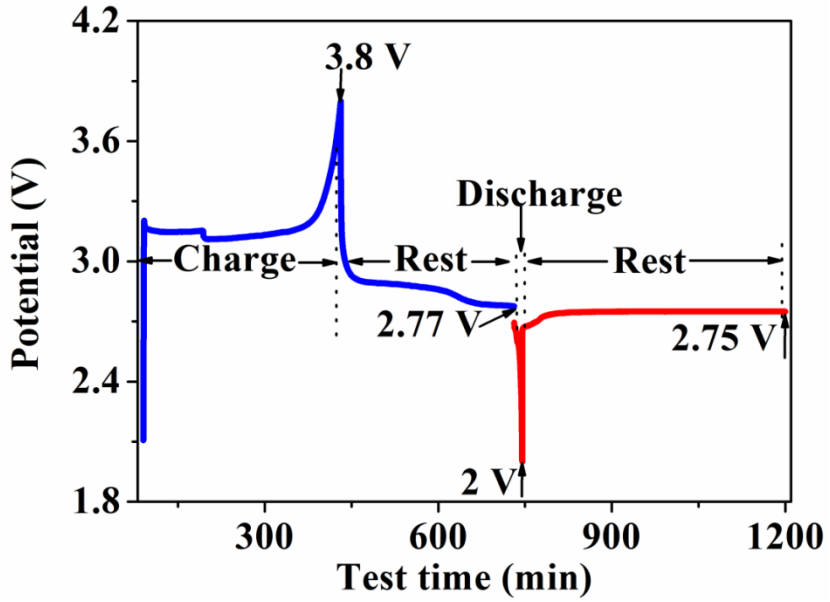

Figure S16. Potential-time profile of LFP//Sn cell. The full cell was charged to 3.8 V (the blue). However, once cutting off external circuit electronics (the rest process), the open circuit voltage immediately drops to 2.77 V from 3.8 V and always maintains at ~2.77 V even for hours, indicating the extracted Li from LFP fails to insert into Sn foil matrix. The real absolute potential of Sn still keeps at a high value. When the cell was discharged, the voltage drops to 2 V from 2.77 V at once and the total process just lasts for ~20 minutes. When the discharge process finishes, the voltage immediately rises to 2.75 V from 2 V and keeps at 2.75 V.

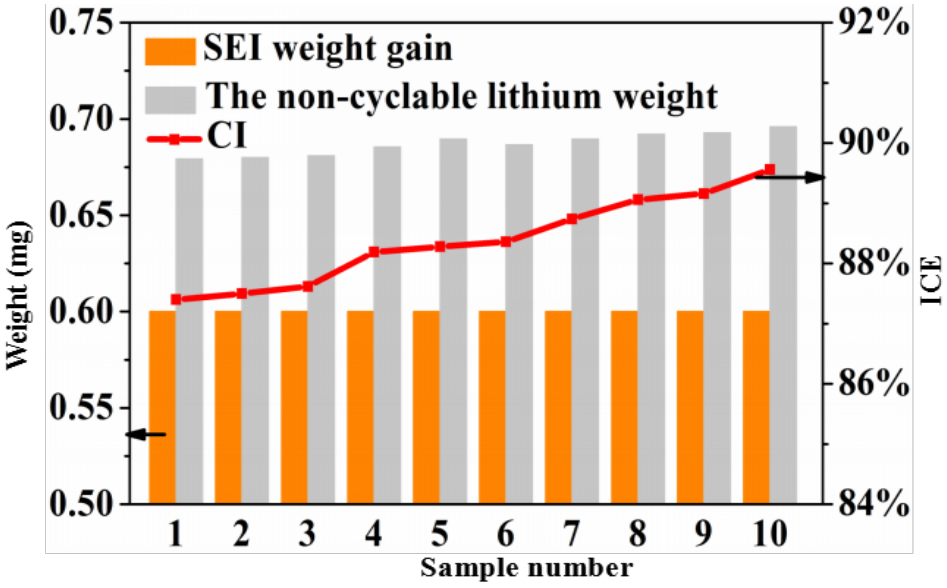

Figure S17. Analysis of SEI weight gain in Sn//Li half-cell. The cells just cycled once. The orange bar is SEI weight gain that is weighed out. The gray bar is the non-cyclable lithium weight that is

theoretically calculated basing on ICE (the red line). It is obvious that the SEI weight is less than non-cyclable lithium weight, which shows that gassing generation takes the upper hand and suppresses the SEI formation during the first cycle.

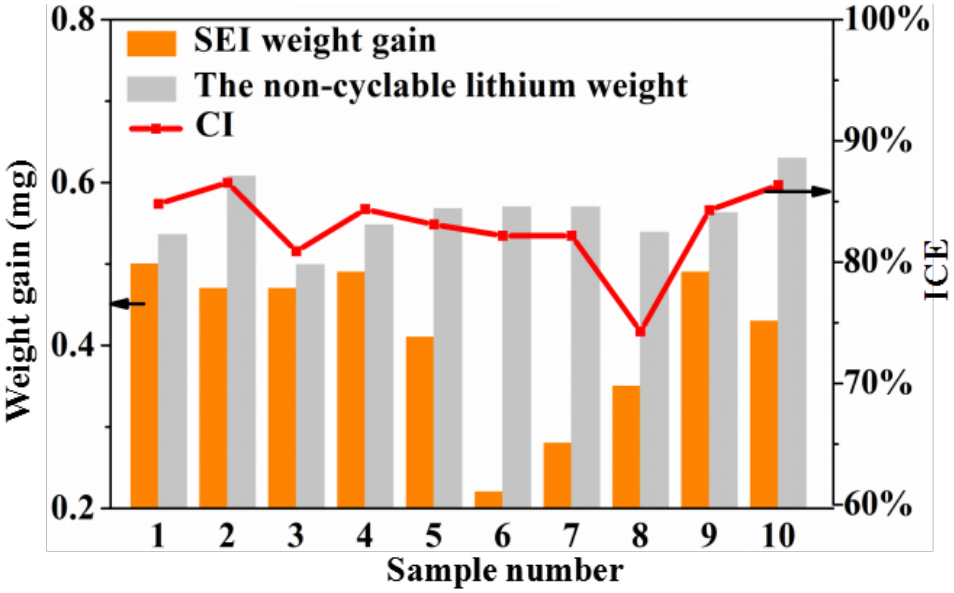

Figure S18. Analysis of SEI weight in LFP//Sn full cell. Note that all cells also were cycled once. The orange bar represents SEI weight gain which is weighed out and the gray bar stands the non-cyclable lithium weight which is calculated basing on ICE (the red). Similarly, the SEI mass of full cell is also less than non-cyclable lithium mass, indicating the serious gassing also happens in LFP//Sn full cell.

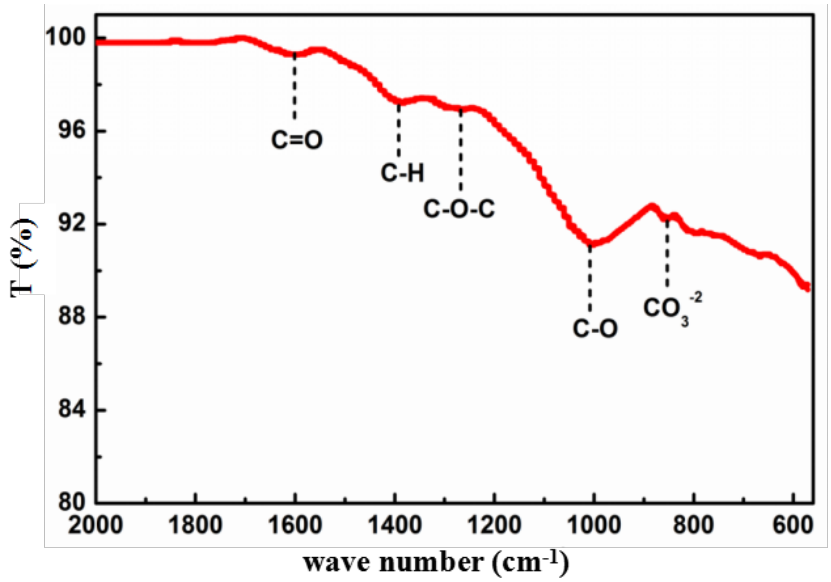

Figure S19. FTIR result of solid products on cycled Sn foil surface. The result reveals the existence of C=O and -C-H, C-O-C at 1600, 1389, 1262 cm^{-1}, respectively. Besides, C-O and CO_3^{-2} also are determined.

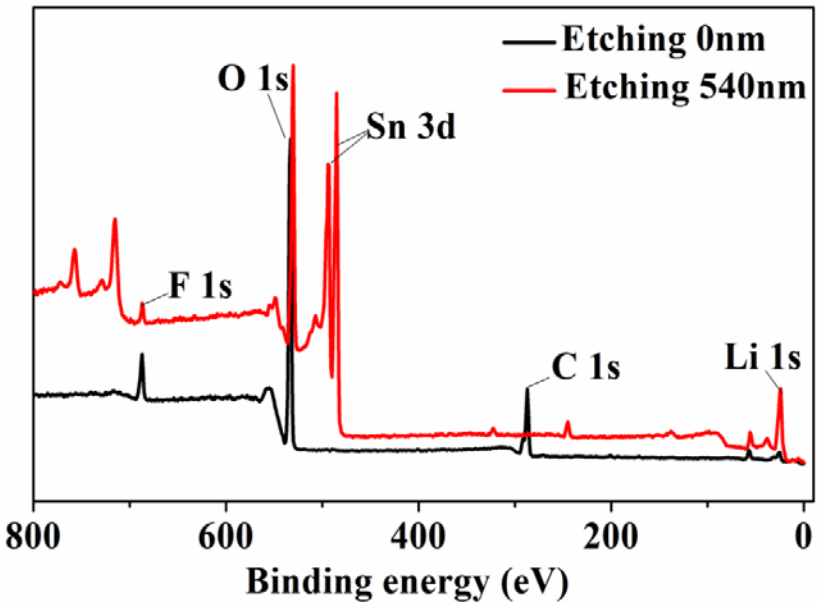

Figure S20. XPS depth analysis result of delithiated Sn foil. The Sn electrode was lithiated and then delithiated in half cell. The black is fresh delithiated Sn and the red is etched. After etching 540 nm (the red), there is still existing high valence Sn.

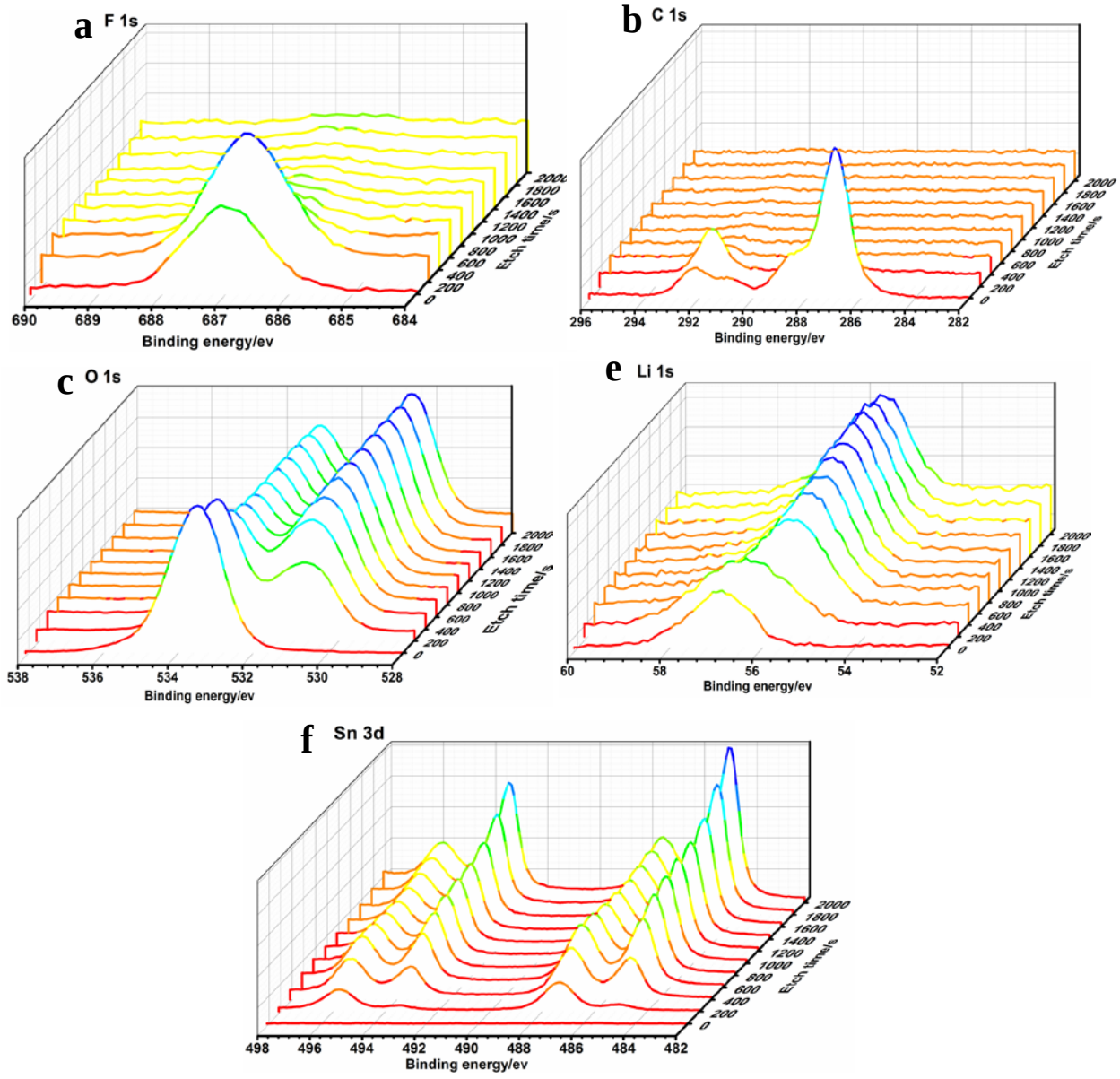

Figure S21. Amount variation of F, C, O, Li and Sn elements were determined by XPS depth analysis technology. The Sn foil electrode was just cycled once.

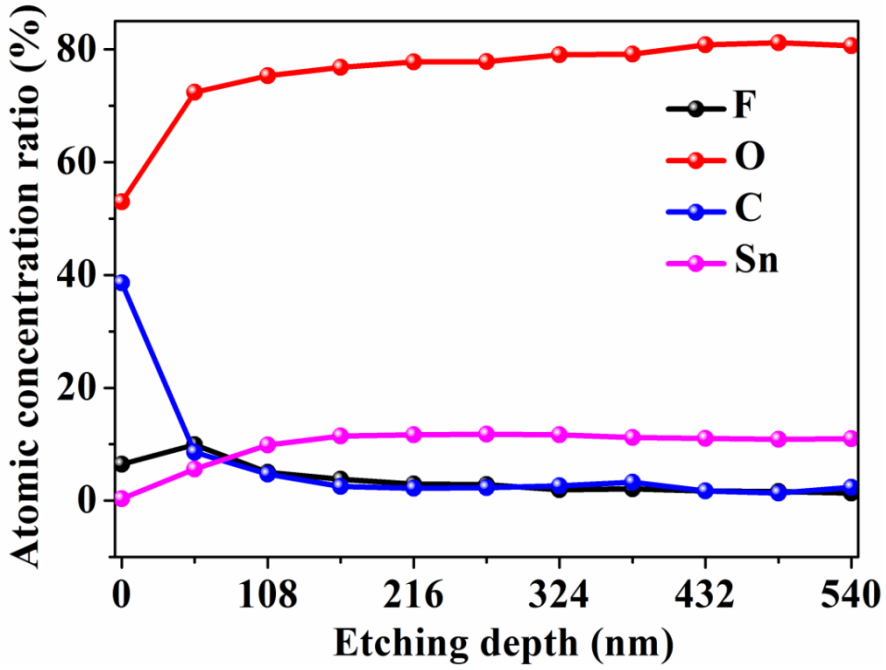

Figure S22. Atomic concentration analysis of the delithiated Sn foil was performed by XPS technology. The cell was tested after 1st cycle. The content of O element always keeps at a higher value than other elements.

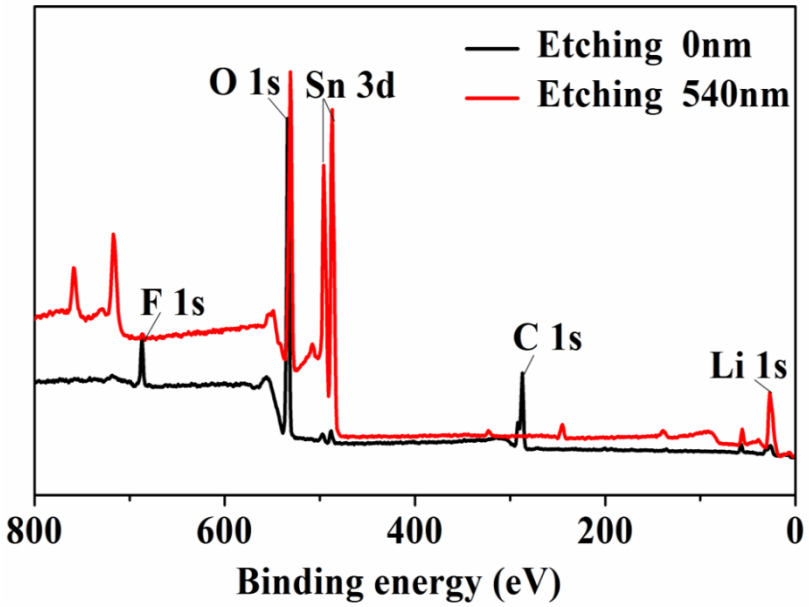

Figure S23. XPS depth analysis result of lithiated Sn foil. The black is fresh lithiated Sn surface. And the red one is etched. There is still Sn of high valence, which implies Sn is involved in SEI formation and generates Sn-F or Sn-F-O bonds.

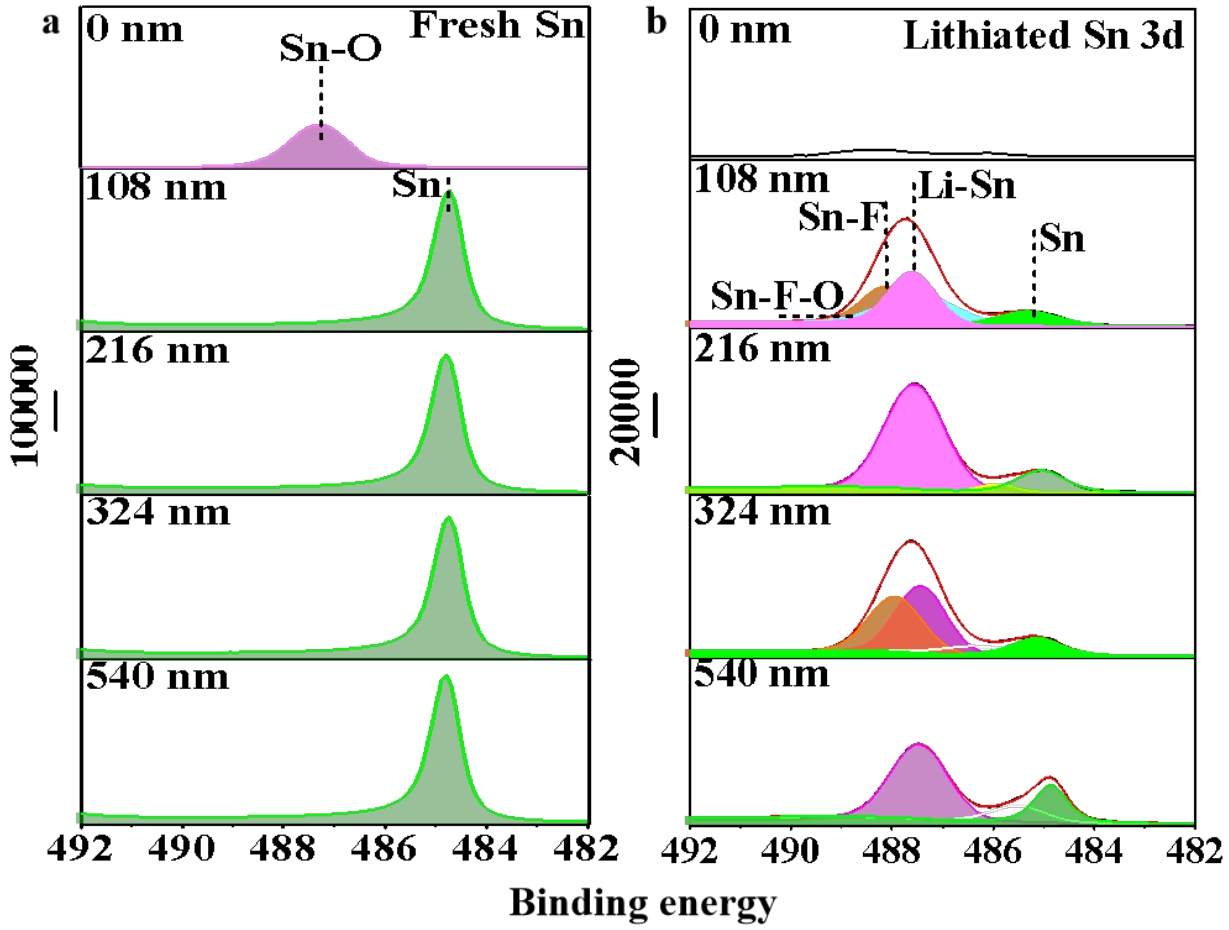

Figure S24. XPS analysis of the fresh Sn and lithiated Sn. a, The fresh Sn foil. The presence of Sn-O is because of the oxidation of pure Sn foil in air. But after etching, only Sn element is detected, which indicates the oxide layer is less than 108 nm. **b,** There is still oxidized tin at 488-487 eV even after etching away 324 nm.

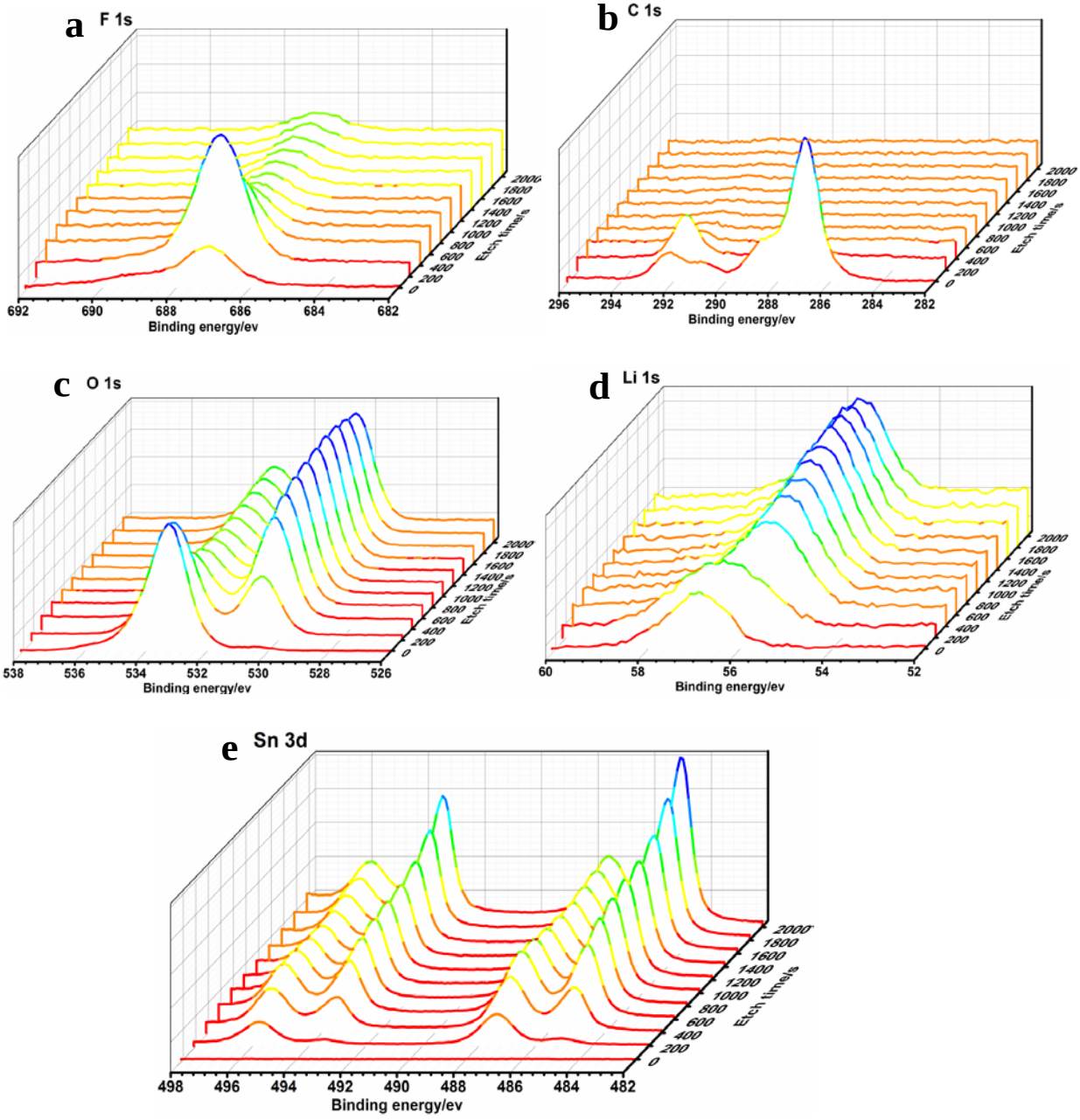

Figure S25. Amount variation of F, C, O, Li and Sn elements of lithiated Sn were determined by XPS depth etching technology.

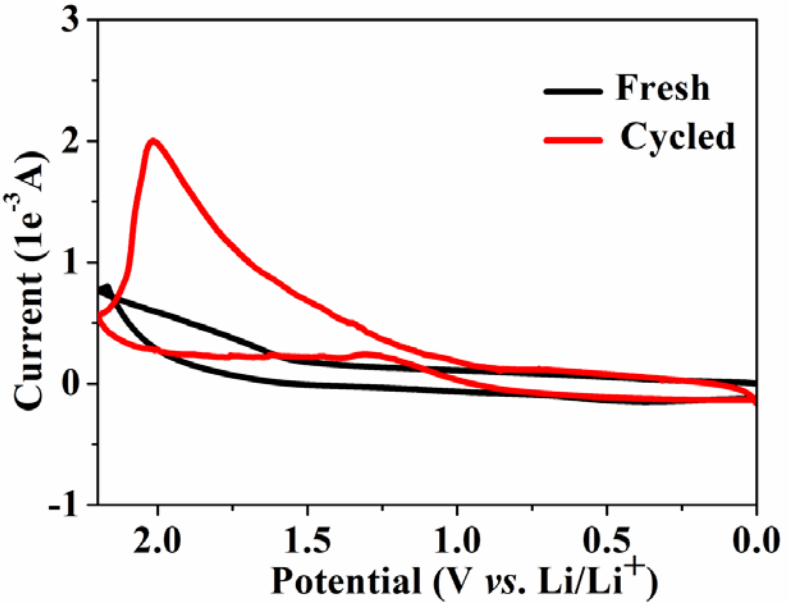

Figure S26. CV analysis of liquid product in Sn//Li half-cell. The black line is steel//Li symmetrical cell, the electrolyte is the fresh 1M $LiPF_6$ in EC/DEC (v/v=1:1) in 10% FEC, 1%VC. The black line almost is a closed straight symmetrical ring, indicating the electrolyte is stable at the range of voltage (0~2.2 V vs. Li/Li^+). The red ring is cycled electrolyte that was extracted from Sn//Li half-cell. The fresh separator dipped the electrolyte and then it was used for assembling steel//Li symmetrical cell. An asymmetrical closed loop indicates there are soluble redox mediators (SRM). The peak located at ~1.9 V vs. Li/Li^+, which attributes to the oxidation of SRM at the voltage.

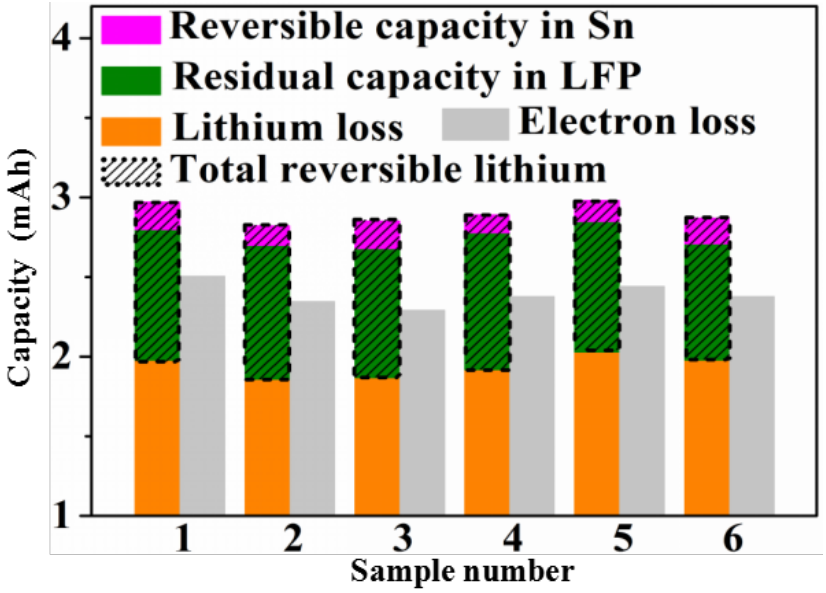

Figure S27. The quantitative analysis of lithium-ion and electron by LFP//Sn full cell. The capacity of LFP cathode (disks with 12 mm diameter) is ~3 mAh. The cyclable lithium is ~0.95 mAh (the slash part) that includes two parts: that can be extracted from Sn (the pink ~0.14 mAh) and residual Li^+ in LFP

(the green ~0.81 mAh). So the real lithium loss is ~1.95 mAh, while the electron loss is 2.31 mAh (based on CE). The number of Li^+ and electron does not match obviously, which is because a part of electrons are consumed for side reactions and soluble redox mediators (SRM).

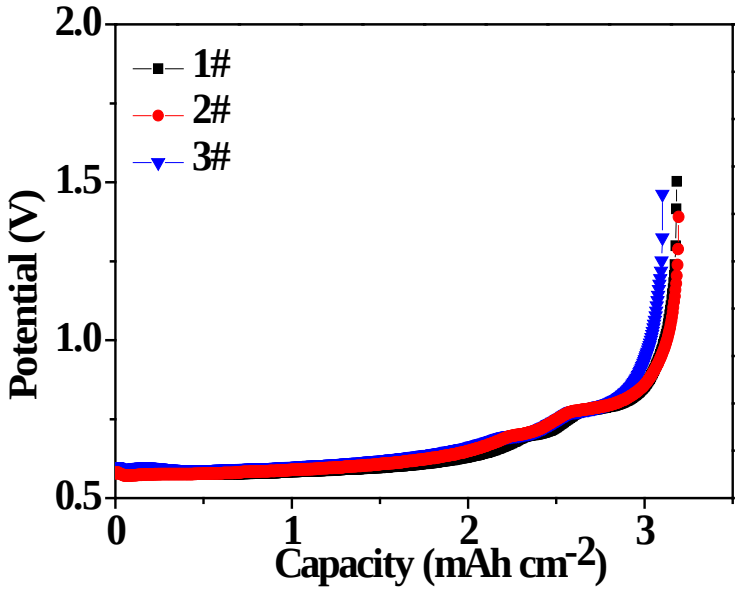

Figure S28. Lithium inventories of Li_xSn foil disks. All delithiation capacity of three disks is ~3.2 mAh cm^{-2}, indicating the excellent uniformity.

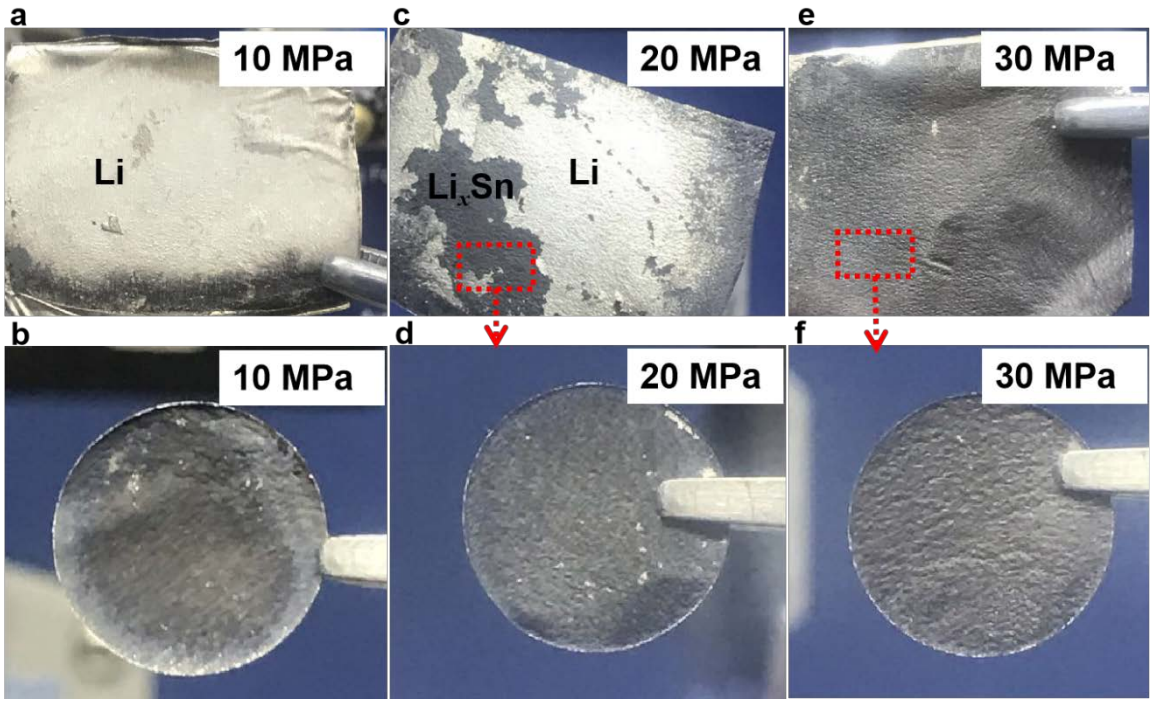

Figure S29. Li_xSn foils were prepared by performing different pressures. a, The prelithiation degree

is low and there is a large amount of unreacted lithium on the surface of Sn foil when the pressure is 10 MPa. **b**, The prelithiation degree was improved and Li_xSn alloy can be obviously found when the pressure increases to 20 MPa, but there is still a thin layer of remaining lithium. **c,** Li foil was totally pressed into Sn matrix and the lithiation uniformity is excellent when the pressure is 30 MPa.

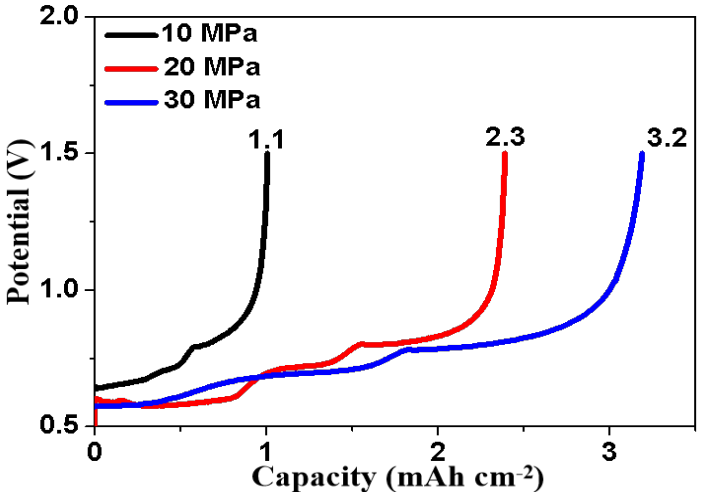

Figure S30. Lithium inventories of Li_xSn foils prepared by different rolling pressures.

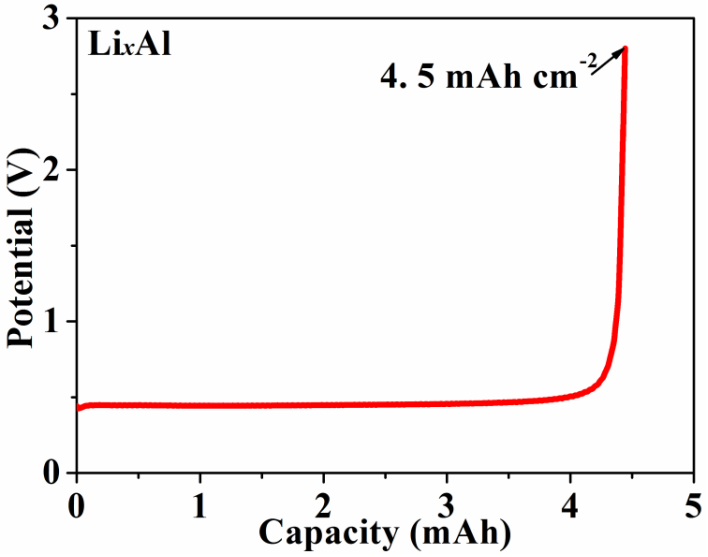

Figure S31. Lithium inventory of Li_xAl foil prepared by mechanical prelithiation method. The capacity of lithium extraction is ~4.5 mAh cm^{-2}, indicating the mechanical prelithiation method also is effective for Al foil prelithiation.

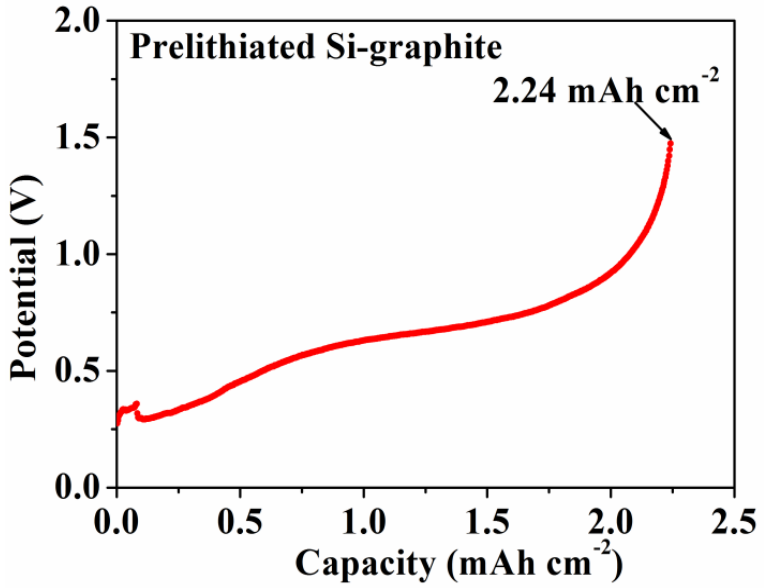

Figure S32. Lithium inventory of Li_xSi/C electrode prepared by mechanical prelithiation method. The capacity of lithium extraction is ~2.24 mAh cm^{-2}, indicating the mechanical prelithiation method also is effective for Si/C electrode prelithiation.

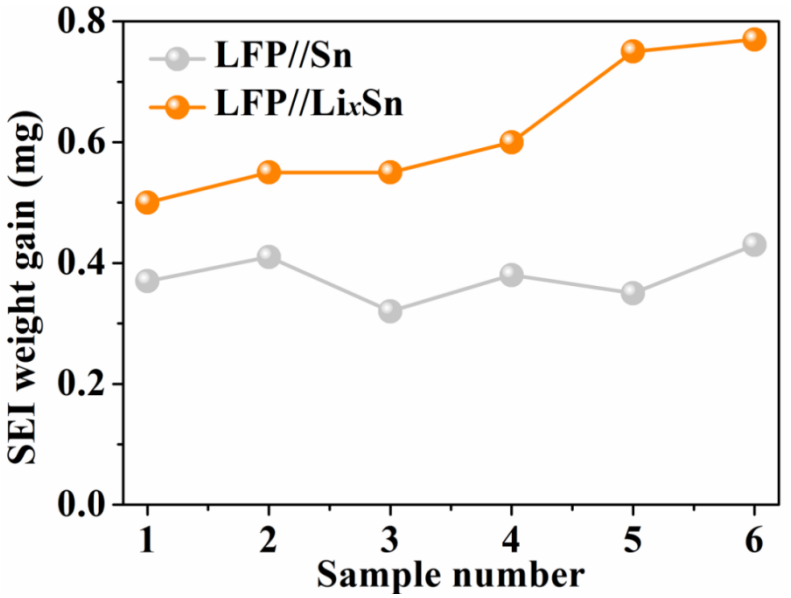

Figure S33. SEI weight gain analysis of LFP//Sn and LFP//Li_xSn cells. The SEI weight gain of Sn foil (the gray) is less than that of Li_xSn foil (the orange), indicating Li_xSn foil indeed can suppress the gassing and help SEI formation.

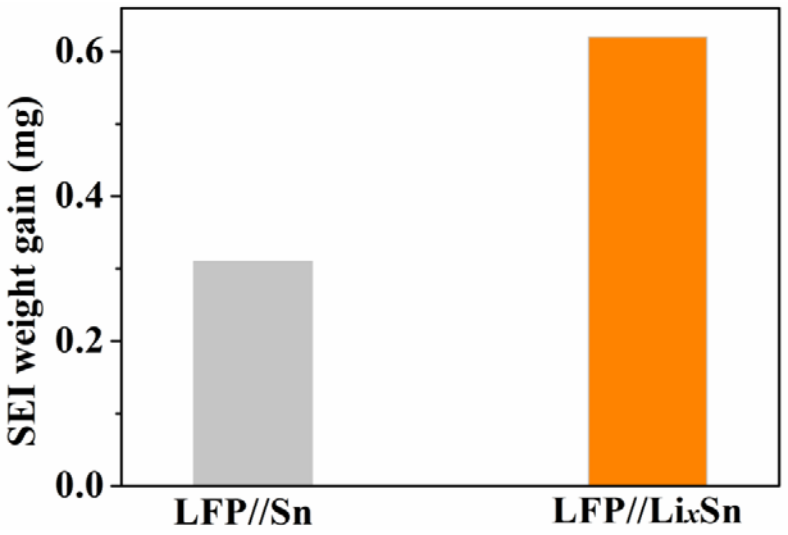

Figure S34. Average SEI weight gain analysis of LFP//Sn and LFP//Li$_x$Sn cells.

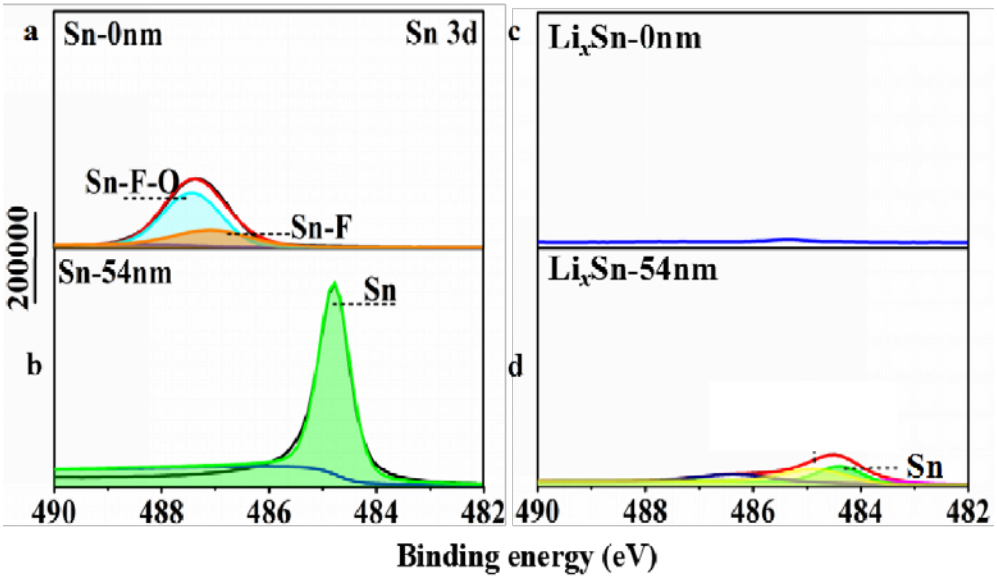

Figure S35. XPS depth analysis result of cycled Sn foil. a,b, Cycled pure Sn foil electrode. The electrode was just cycled once. The peak of cycled pure Sn foil mainly located at ~487 eV (a). After etching 54 nm, the peak is mainly located at ~485 eV, which is attributed to Sn elements. (b). **c,d,** Cycled Li$_x$Sn foil electrode. However, only rare Sn element can be detected in Li$_x$Sn because more compact SEI formed (c). Besides, after etching 54 nm (the pink), some weak Li-Sn and Sn peaks were detected and there are no peaks of Sn-F or Sn-F-O, indicating the dense SEI forms rapidly and hinders Sn involving in parasitic reactions.

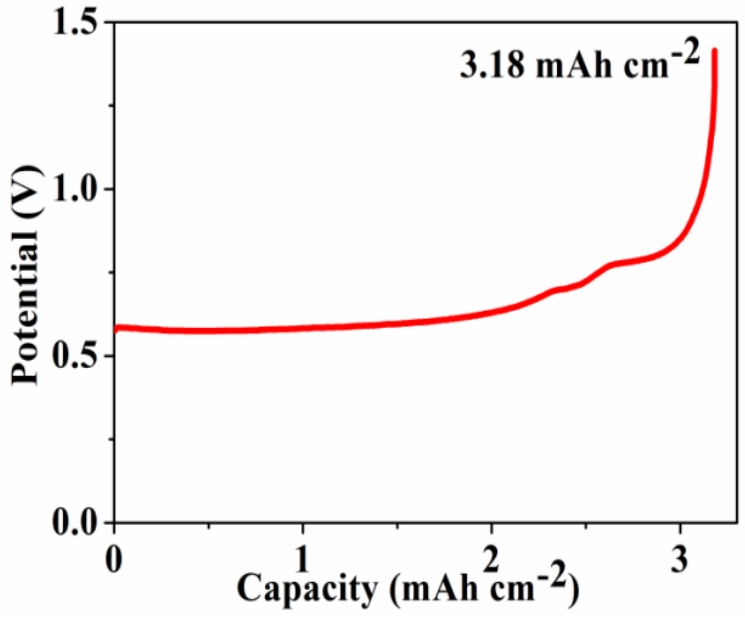

Figure S36. Lithium inventory of Li_xSn prepared by mechanical prelithiation method.

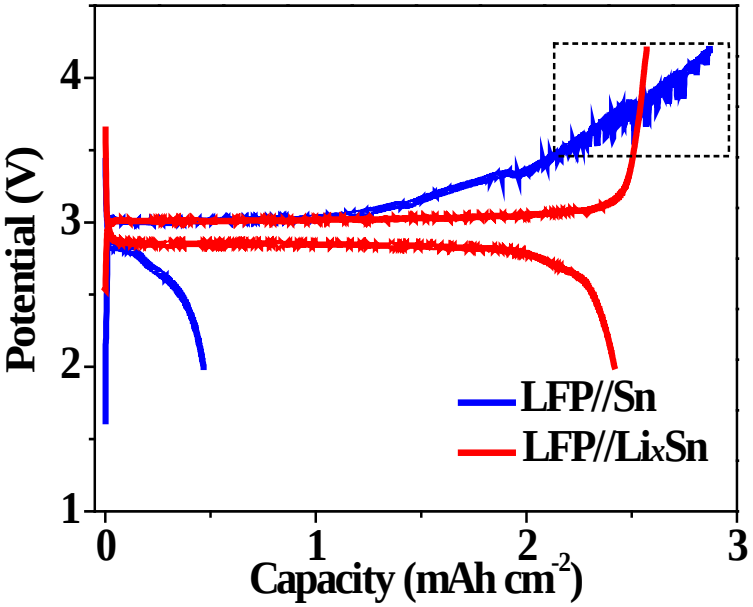

Figure S37. Voltage-capacity profiles of LFP//Sn and LFP//Li_xSn cells. The blue is LFP//Sn and the red is LFP//Li_xSn. The fluctuating potential at final charge stage (the blue) may be caused by gassing. But the red is quite stable and smooth, indicating Li_xSn can effectively suppress the side reactions.

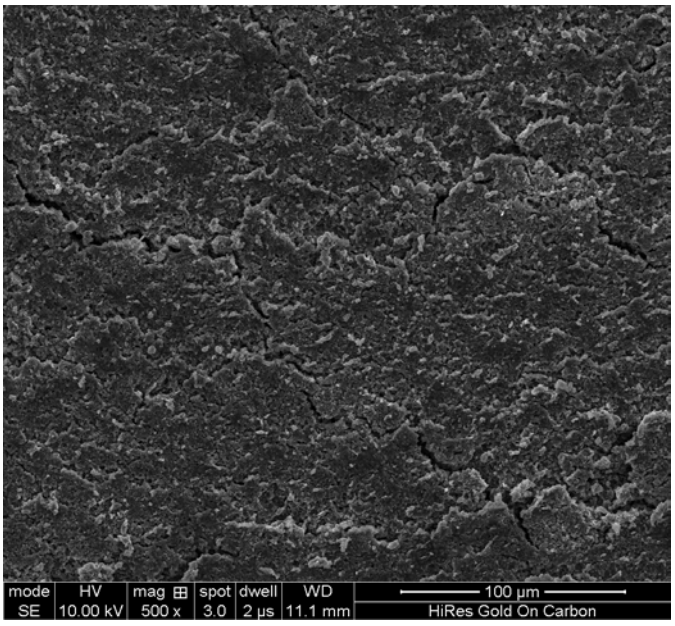

Figure S38. Surface characterization of cycled Li_xSn foil. There are no bubble footprints, indicating the gassing behavior was suppressed. The scattered cracks were most likely caused by the large volume expansion.

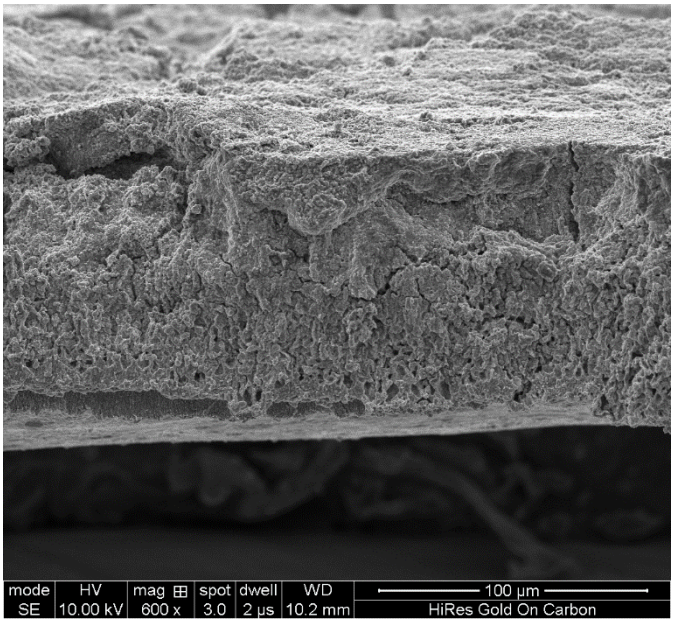

Figure S39. Cross-sectional observation of cycled Li_xSn electrode. The denser structure and loss of electrode damage benefit from the rapid SEI formation and relatively smaller volume change of Li_xSn.

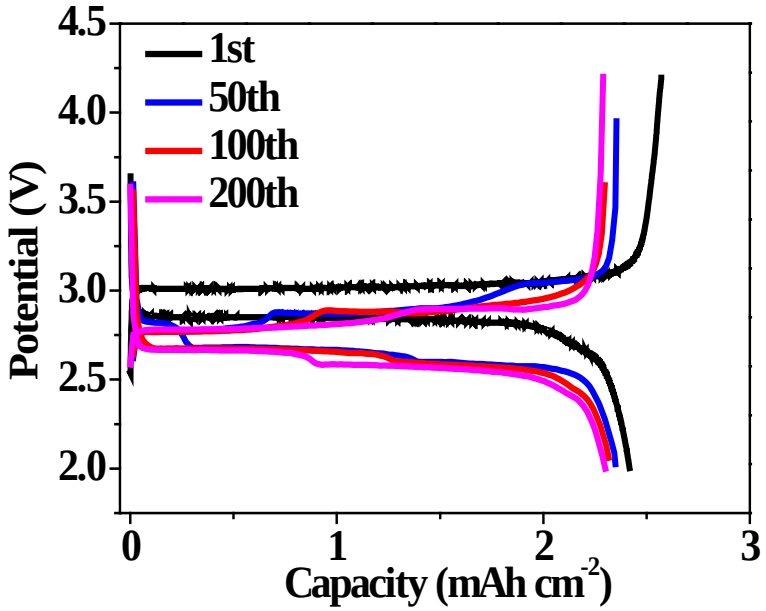

Figure S40. Voltage-capacity curve of LFP//Li$_x$Sn cell. The curves of 100th and 200th almost are completely overlapping, indicating the stable performance of LFP//Li$_x$Sn.

Table S1. Coulombic efficiency of composite Sn materials from reported literatures

	ICE/%	Averange CE/%	Cycle numbers	Capacity (mAh/g)	Current density	Active material loading (mg)
Sn/C[1]	69	100 after 10 cycles	130	710	0.25C	1.0
Sn@C[2]	61	98~100 from the 30th	500	810	0.2C	1
Sn/NC[3]	48	>99	400	630	0.2A/g	0.8−1.0
Sn@G-PGNWs[4]	69	96.3	1000	682	2A/g	1
Sn@HC[5]	71.9	100 after the third cycle	6000	423	4A/g	1.5~2.0
Sn/NRGO[6]	95	---	100	755	100mA/g	1.7~3.8
Ni–Sn[7]	60	---	400	700	0.2C	1.09
CoSn$_2$/a-TiC/C[8]	83.2	---	180	365	3C	2.4

Table S2. Fitting resistance result of half-cell with different cycles

	R_0/Ω	R_1/Ω
Fresh	2.656	41.11
Resting for 12h	2.331	73.22
1st	2.378	564.3
3rd	2.367	1571
5th	2.384	1335
10th	2.965	107.3
15th	4.223	186.3
20th	5.044	218.9
Reassemble	2.677	103.4

R_0 is the interface impedance of Li metal and electrolyte. With the reaction, R_0 is slightly decreased to 2.384 from 2.656 Ω and afterwards R_0 increase to 5 from 2.384 Ω again. R_1 is interface impedance of Sn foil and electrolyte. Once discharged, the resistance increases to 564.3 from 73.22 Ω, which is due to gassing dewetting electrolyte. And the subsequent cycles (from 3rd to 5th cycle), the gassing intensifies and R_1 further rises, even is up to 1335 Ω. And after 5th cycle, the decreased R_1 indicates the gassing behavior gradually weakens.

Table S3. Li–Sn compounds and corresponding capacities and electrode potentials

	Theoretical capacity（mAh/g）	**Potential (V *vs.* Li/Li^+)**
Li_2Sn_5	88.3	0.760
LiSn	213.3	0.660
Li_3Sn_2	-	-
Li_5Sn_2	492.5	0.485
$Li_{13}Sn_5$	509.6	0.485
Li_7Sn_2	656	0.420
Li_4Sn	-	-
$Li_{22}Sn_5$	790	0.380

Supplementary Video

Video S1: In-situ X-ray synchrotron radiation

http://li.mit.edu/S/HuiXu/Upload/VideoS1-In-situX-raysynchrotronradiation.mp4

Video S2: Bubbles of visual cell

http://li.mit.edu/S/HuiXu/Upload/VideoS2-Bubble-visualcell.mp4

Supplementary references

1. Yun X. et al. Uniform Nano-Sn/C Composite Anodes for Lithium Ion Batteries. Nano Letters **13**,470-474(2013).

2. H. Zhang. et al. Tailored Yolk-Shell Sn@C Nanoboxes for High-Performance Lithium Storage. Adv. Funct. Mater **27**,1606023(2017).

3. Duck H Y. et al. Simple Synthesis of Nanostructured Sn/Nitrogen-Doped Carbon Composite Using Nitrilotriacetic Acid as Lithium Ion Battery Anode. Chemistry of Materials **28** (5), 1343-1347(2016).

4. Jian Q. et al. Graphene Networks Anchored with Sn@Graphene as Lithium Ion Battery Anode. ACS Nano **8** (2),1728-1738(2014).

5. Ning Z. et al. Ultrasmall Sn nanoparticles embedded in spherical hollow carbon for enhanced lithium storage properties. Chem.Commun **54**,1205-1208(2018).

6. Jarulertwathana, N. et al. Nano-structure tin/nitrogen-doped reduced graphene oxide composites as high capacity lithium-ion batteries anodes. J Mater Sci: Mater Electron **28**: 18994(2017).

7. Jun L. et al. Facile Synthesis of Highly Porous Ni-Sn Intermetallic Microcages with Excellent Electrochemical Performance for Lithium and Sodium Storage. Nano Letters **14** (11), 6387-6392(2014).

8. Min-Gu P. et al. Sn-Based Nanocomposite for Li-Ion Battery Anode with High Energy Density, Rate Capability, and Reversibility. ACS Nano **12** (3), 2955-2967(2018).